Ion source studies at the ORNL ECR source facility

F. W. Meyer and J. W. Hale

Oak Ridge National Laboratory, Oak Ridge, Tennessee 37831-6372

CONF-890703--11

DE89 014881

Abstract

Using high resolution magnetic analysis, we have measured energy spreads of Ar^{+q} ($1<q<12$) ion beams extracted from the ORNL ECR ion source under a number of different ECR plasma conditions. The measured energy spreads for the different charge states fall in the range 8 to 20 eV per charge and are all roughly proportional to the ion charge. In addition, we have used a combination of magnetic and electrostatic analysis to investigate the high charge state tail of the extracted Ar^{+q} charge state distribution. Charge states up to +16 have been positively identified; in addition, tentative identification of extracted Ar^{+17} ions has been made, with total intensity in the range 10 to 20 kHz.

Introduction

In this paper we report on recently performed studies at the ORNL ECR ion source facility of two issues of Ar^{+q} ion beam production: the energy spreads of extracted ion beams, measured under different plasma conditions, and the highest extracted Ar charge state obtainable with our 10.6 GHz ECR ion source. The first issue, although addressed already earlier,[1,2] has recently received renewed attention[3] in connection with the gas mixing effect observed almost universally in ECR sources. The second issue is of interest primarily because of the atomic physics applications of ECR sources, but also in order to permit a more quantitative comparison between lower-frequency-ECRIS and EBIS performance. In this context it is noted that Geller[4] has recently reported 1 enA extracted Ar^{+18} ion beam intensity for the 16.6 GHz MINIMAFIOS source.

Apparatus and Procedure

Figure 1 shows the salient features of the experimental configuration used for the present measurements. The energy spread measurements were obtained using the double-focusing main charge analyzing magnet (B1 in Fig. 1) with 1 mm and 2 mm entrance and exit slits in the dispersing and orthogonal planes, respectively. Energy spreads were inferred from the widths of 1 keV x q ion beam profiles which represent the current transmitted through slit SL2 measured in FC2 as a function of analyzing magnetic field. From detailed slit width dependence measurements, it was determined that, for the above slit settings, the ion energy spread dominates the observed profile widths. Results

of such a slit width study are illustrated by the solid triangles in Fig. 2. For large slit openings (i.e., beyond about 6 mm), where the beam profile FWHM is dominated by the instrumental FWHM of the analyzing magnet, the measured widths fall systematically below those expected from the theoretical FWHM analyzer resolution[5] (dashed line in Fig. 2) given by $dB/B = 1/2(s_{en} + s_{ex})/(4r_0)$, where s_{en} and s_{ex} are the analyzer entrance and exit slit widths, respectively, and r_0 the analyzer radius of curvature (40 cm). This weaker slit width dependence occurs when the image of the plasma aperture no longer fills the analyzer entrance aperture, at which point the effective entrance aperture becomes constant and independent of the physical slit opening. This interpretation is supported by measurements carried out using an 80 keV Ar^{+8} ion beam, shown as the solid squares in Fig. 2, which show a similar weakening of the slit width dependence beyond about 6 mm. At this higher energy the measured widths are completely dominated by the instrumental function over the whole range of slit widths investigated.

The study of the high charge-state tail of the Ar^{+q} charge state distribution was carried out using a parallel plate electrostatic analyzer (EA in Fig. 1) operated in particle counting mode and located at the focal plane of a half scale version of the main charge analyzer, which is normally used as a deflection magnet to direct beam to beamlines 2-4. A gas cell located between deflector B2 and analyzer EA permits charge assignment of the primary ion beam through identification of the electron capture components exiting the cell. The m/q analysis provided by B1 and B2, the E/q analysis provided by EA, and the q analysis made possible by use of charge exchange collisions in GC combine into a

powerful diagnostic for determining the various constituents with (near) identical momentum per charge ratios present in a selected ion beam.

Energy Spread Measurements

Figure 3 summarizes the present results for the energy spreads (in units of eV per unit charge) observed for a range of Ar charge states under a variety of different source conditions. The solid circles were obtained subsequent to source optimization of Ar^{+9} without O_2 mix gas. Extraction potential and source conditions were held constant for the other charge states, while small adjustments were made in einzel lens setting and steering. The open circles represent the energy spreads obtained subsequent to optimization of Ar^{+9} with O_2 mix gas. Finally, for the open triangles, each charge state was individually optimized with respect to r.f. power, source pressure, Ar/O_2 mix ratio, and solenoidal field profile.

Since the observed spreads are all roughly proportional to charge (i.e., the reduced energy spreads are roughly constant) the dominant broadening mechanism must be related to the plasma potential distribution and not the ion kinetic energy distribution in the ECR plasma, as has been recently suggested.[3] This conclusion is consistent with explicit ion temperature measurements[1] using a retarding potential technique, which showed that the ion temperature is indeed small compared to the extracted beam energy spread.

The use of O_2 mix gas does seem to decrease the observed energy spreads of extracted Ar ion beams, as has recently been observed by Antaya.[3] The mechanism

responsible for this effect, however, is more likely to be a modification of the plasma potential distribution by the mix gas (either directly or via the neutral gas density or the electron density) than the recently proposed[3] ion "cooling" by the light mixing gas. Figure 4 shows that changes in source pressure and/or r.f. power can significantly affect observed energy spreads. In addition, although not shown in Fig. 4, we have observed a 50% increase in energy spread when increasing the extraction voltage from -100 V to -1 kV for 8 keV Ar^{+8} beams. Such dependence on extraction voltage has been previously described.[1]

Finally, it is noted that current optimization of a particular extracted high charge state beam does not necessarily imply a minimization of energy spread. For example, even though three times as much Ar^{+12} beam intensity is obtained from an Ar^{+12} optimized plasma as from an Ar^{+9} optimized plasma, the observed Ar^{+12} energy spread is 50% larger than that observed for the Ar^{+9} optimized case.

High-q Tail of the Ar Charge State Distribution

One of the problems associated with positive identification of extracted ion beams using purely magnetic analysis is accidental near or exact mv/q degeneracies with contaminant beams. The problem becomes more significant when investigating the high-q tails of charge distributions, where the intensities of the beams of interest are weak, i.e., of the same order as those of the contaminant beams. Ar^{+16} is a good example of this situation. This Ar charge state has the same m/q as charge state +6 of ^{15}N, which is

always present in minute quantities in ECR sources, due to the 0.37% natural abundance of this isotope. This contaminant is clearly identified by its 6-5 charge transfer component in the parallel plate analyzer scan shown in Fig. 5. Also clearly identifiable in that scan are the 16-15 and 15-14 charge transfer components of Ar^{+16}. The presence of the second charge transfer component indicates the occurrence of multiple collisions in the gas cell. From the known intensities of the charge transfer components, the known cell target thickness and relevant cross sections,[6] the intensities of Ar^{+16} and $^{15}N^{+6}$ in the primary beam entering the gas cell can be determined. Typical values are 50 kHz and 75 kHz for Ar^{+16} and $^{15}N^{+6}$, respectively. From measurements performed with Ar^{+13} to determine the fraction of the total source output transmitted through the beam limiting 1 mm x 2 mm magnetic analyzer slits, the total source output of Ar^{+16} is inferred to be about 4 MHz. The small peak at about 7 kV analyzer voltage to the left of the primary beam in Fig. 5, is identified as an O^{+6} beam that has lost about 6% of its energy during grazing-angle scattering on slits SL1. Since such straggling results in a broad range of final energies, this mechanism produces a continuum of magnetic rigidities; such contaminants can therefore be present over a relatively wide range of magnetic analyzer settings.

Figure 6 shows an electrostatic analyzer scan for B1 and B2 set to transmit beams with m/q = 40/17. From the charge transfer components present, it is inferred that the primary beam consists of Ar^{+17} and F^{+8} with m/q ratios of 2.3529 and 2.3750, respectively. Using the technique described in the previous paragraph, a maximum source output of 10 to 20 kHz is estimated for Ar^{+17}. We note that source optimization for both Ar^{+16} and

Ar^{+17} was accomplished by tuning on the charge transfer components. It is speculated that the reason for our inability to resolve the above two components is due to the increased energy spread when optimizing on the higher Ar charge states, as already suggested in Fig. 2. Extrapolating on the basis of the trend established for +11 and +12 (open triangles in Fig. 2) an estimate of ~20 eV/q is obtained for the energy spread of Ar^{+16}, which is sufficient to prevent complete resolution of Ar^{+17} and F^{+8}. The uncertainty of this extrapolation makes our identification of Ar^{+17} more speculative than that of Ar^{+16}. An additional source of uncertainty in our identification is shown in Fig. 7. When extending the analyzer scan to lower voltages, a straggling peak is found at about 6.63 kV, which, similar to the Ar^{+16} case, is identified as O^{+6} lowered in energy by about 12% by slit scattering. We note parenthetically that to increase slit lifetimes, our analyzing slits were machined with square instead of knife edges, which increases the probability of slit scattering. If the identification of this straggled component is correct, then its 6-5 charge transfer component is located at the same analyzer voltage setting as the 17-16 charge transfer component of Ar^{+17}. We cannot exclude the possibility that the straggled O^{+6} component contributed to the 17-16 component shown in Fig. 6. As has been shown by Geller,[4] a positive identification of H-like and fully stripped Ar ions is possible by the detection of characteristic K shell X rays produced during low energy ion-atom or ion-surface collisions. This technique, however, is less straightforward to implement for quantitative measurements, which we find to be an attractive feature of the present

approach. Plans are underway to repeat the above measurements after installation of knife-edged slits.

Acknowledgments

The authors dedicate this paper in memory of C. F. Barnett as acknowledgment of invaluable guidance over the years. Illuminating discussions with R. A. Phaneuf are gratefully acknowledged. This work was supported by the Office of Fusion Energy, U.S. Department of Energy, under contract No. DE-AC05-84OR21400 with Martin Marietta Energy Systems, Inc.

References

1. H. Koehler, M. Frank, B. A. Huber, and K. Wiesemann, Contributed Papers of the 7th Workshop on ECR Ion Sources, 22-23 May, 1986, ed. by H. Beuscher, Juelich Report No. ISSN 0344-5798, p. 215.

2. F. W. Meyer, op. cit., p. 11; the erroneous instrumental width quoted therein (p. 21) is a factor of two too large, resulting in an underestimate of the quoted ion energy spreads.

3. T. A. Antaya, J. de Phys. 50, C1-707 (1989).

4. R. Geller, F. Bourg, P. Briand, J. Debernardi, M. Delaunay, B. Jacquot, P. Ludwig, R. Pauthenet, M. Pontonnier, and P. Sortais, Proceedings of the International Conference On ECR Ion Sources and their Applications, 16-18 Nov. 1987, ed. by J. Parker, NSCL Report No. MSUCP-47, p. 1.

5. e.g., P. Grivet, Electron Optics, Pergammon Press, Oxford, 1972, p. 348.

6. e.g., H. Tawara, T. Kato, and Y. Nakai, "Electron Capture and Loss for Collisions between Heavy Ions and Hydrogen Molecules", IPPJ-AM-28, Nagoya University, Nagoya, Japan, 1983.

Figure Captions

Fig. 1. Schematic diagram of the experimental configuration; L1, L2 - einzel lenses; ST - magnetic steering; SL1 and SL2 - slits; FC1, FC2, and FC3 - faraday cups; B1 and B2 - double-focusing analyzing magnets; GC - gas cell; EA - parallel plate analyzer; BL1, BL2, BL3, BL4 - beam lines.

Fig. 2. Measured beam-profile FWHM as a function of analyzer slit width for 8 keV Ar^{+8} ions (triangles), 80 keV Ar^{+8} ions (squares); dashed line is the theoretical instrumental profile FWHM.

Fig. 3. Measured energy spreads vs. argon charge state; solid circles - plasma optimized for Ar^{+9} without O_2: 210W rf power, 2.5 x 10^{-6} Torr source pressure; open circles - plasma optimized for Ar^{+9} with O_2: 195W rf power, 3 x 10^{-6} Torr source pressure, 2/5 Ar/O_2 mix ratio; open triangles - each charge state individually optimized.

Fig. 4. Ar^{+1} ion profiles measured for different source conditions.

Fig. 5. Electrostatic analyzer scans after magnetic m/q selection 40/16 with and without gas in the charge transfer cell.

Fig. 6. Electrostatic analyzer scan after magnetic m/q selection 40/17 with gas in charge transfer cell (indicated pressure is beam line pressure).

Fig. 7. Extended electrostatic analyzer scan after 40/17 magnetic m/q selection, showing straggling O^{+6} peak at 6.63 kV.

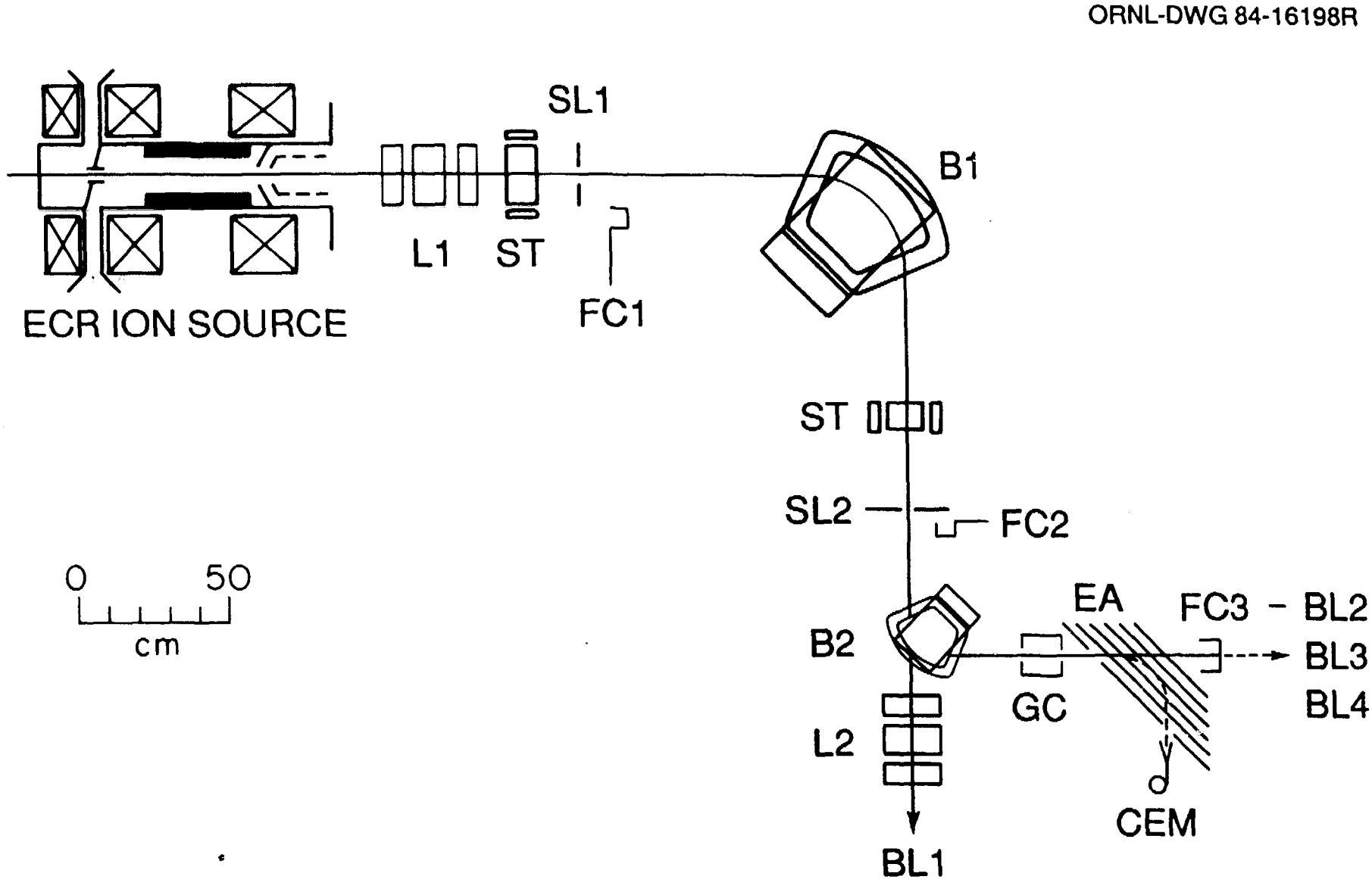
ORNL-DWG 84-16198R
SL1
B1
L1
ST
FC1
ECR ION SOURCE
ST
SL2
FC2
0
50
cm
EA
FC3 - BL2
B2
BL3
BL4
GC
L2
CEM
BL1

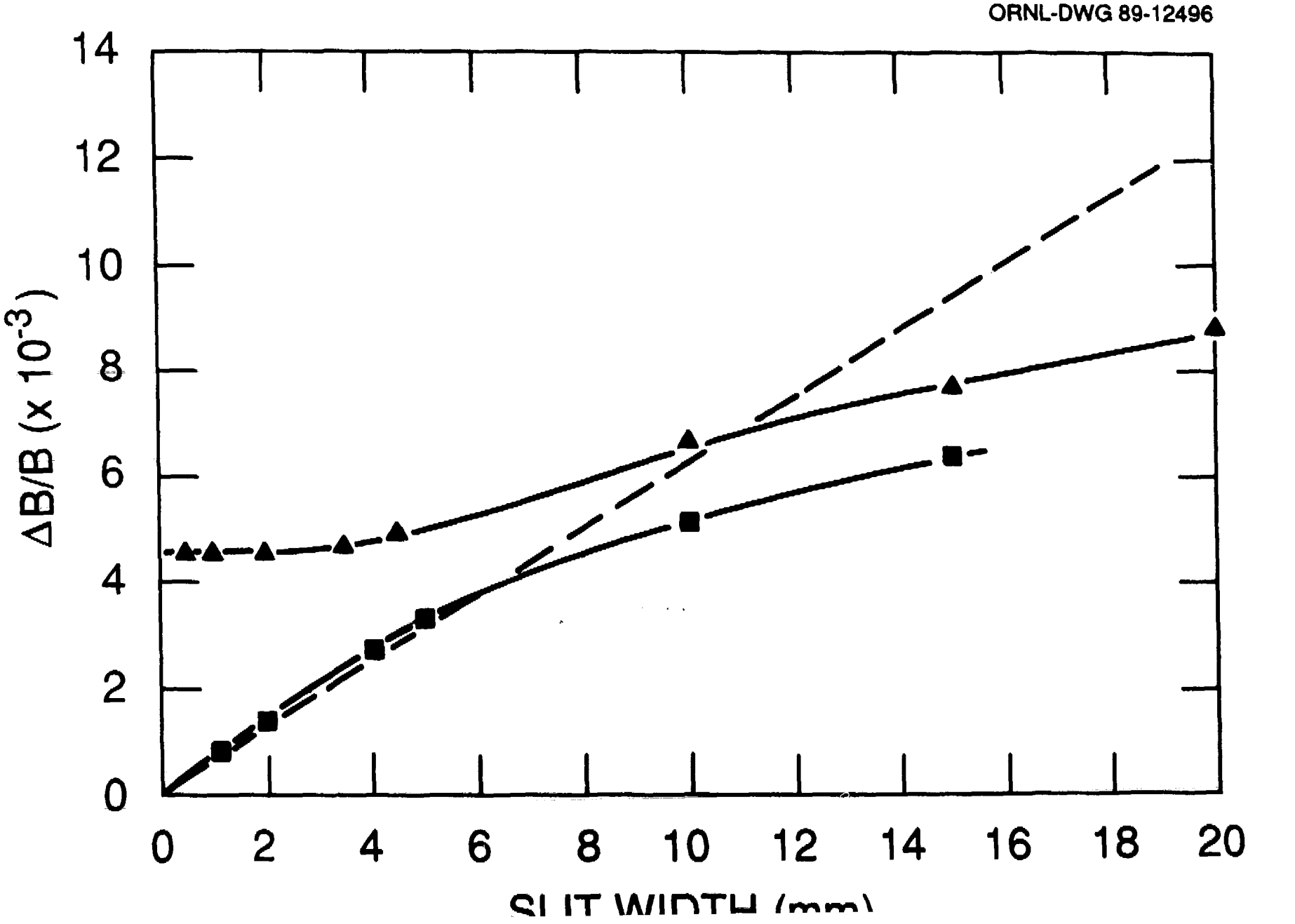
ORNL-DWG 89-12496
14
12
10
8
6
4
2
0
ΔB/B (x 10-3)
0
2
4
6
8
10
12
14
16
18
20
SLIT WIDTH (mm)

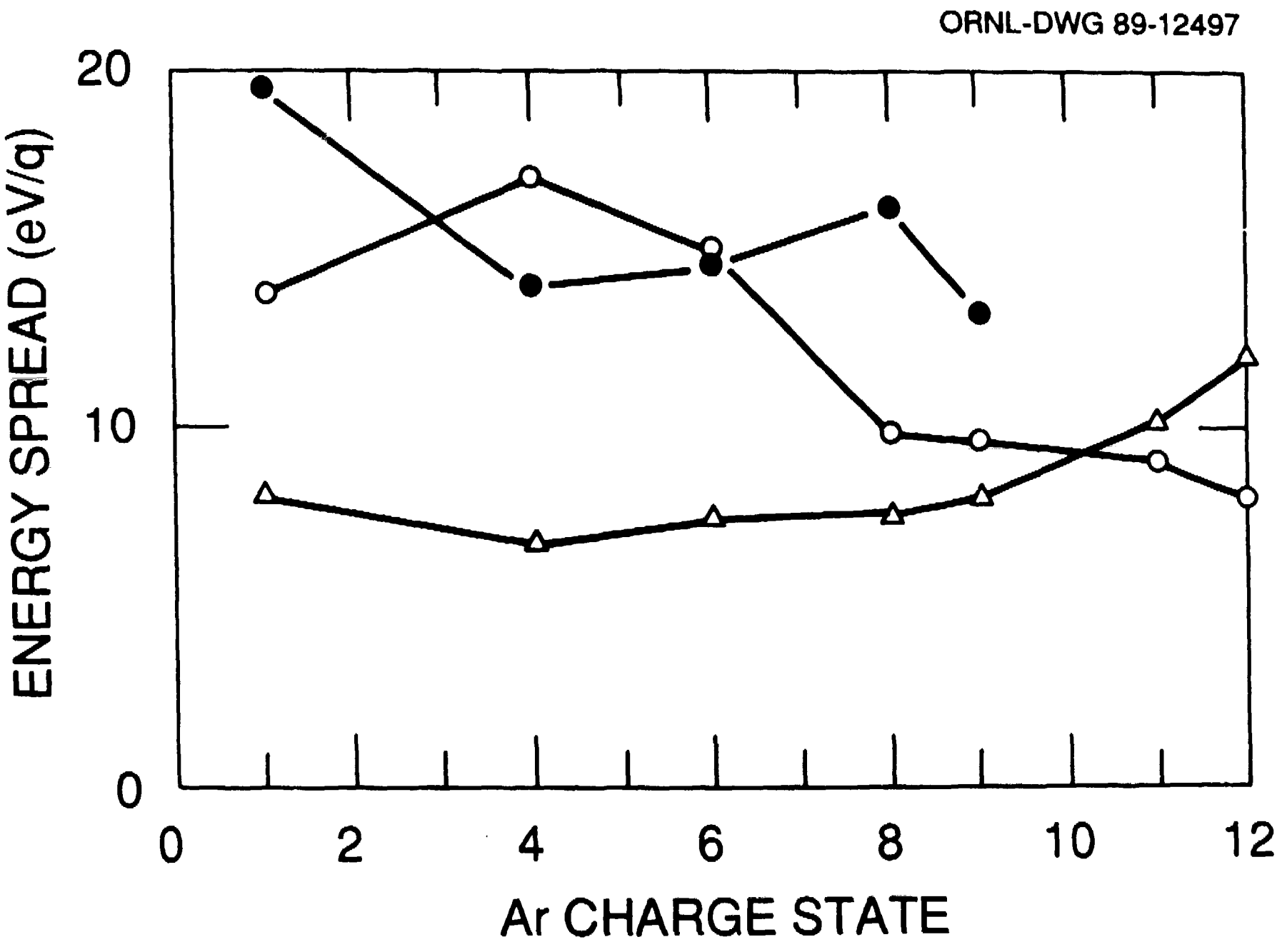
ORNL-DWG 89-12497
20
10
0
ENERGY SPREAD (eV/q)
0
2
4
6
8
10
12
Ar CHARGE STATE

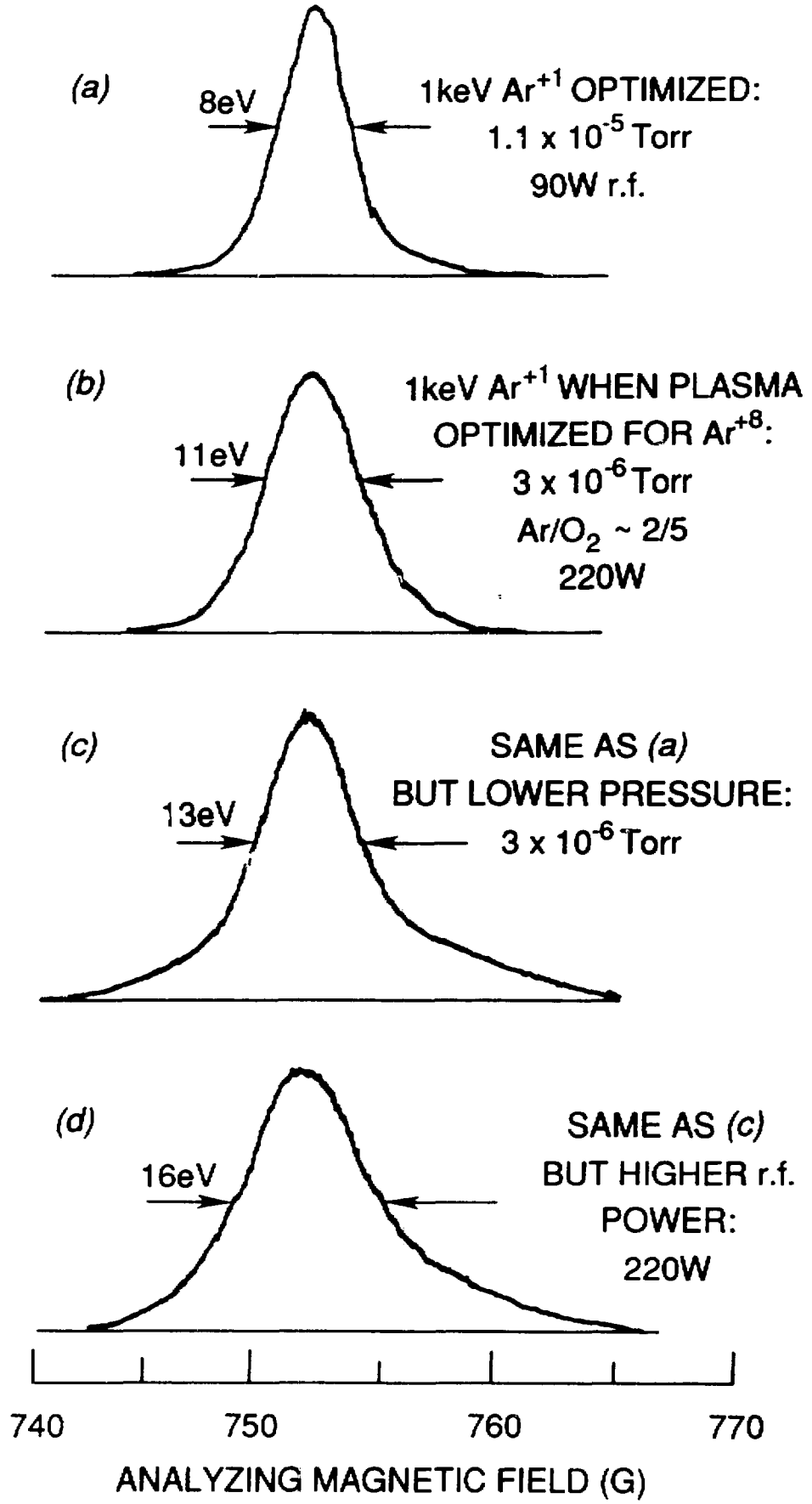
(a)
8eV
1keV Ar+1 OPTIMIZED:
1.1 x 10-5 Torr
90W r.f.
(b)
11eV
1keV Ar+1 WHEN PLASMA
OPTIMIZED FOR Ar+8:
3 x 10-6 Torr
Ar/O2 ~ 2/5
220W
(c)
13eV
SAME AS (a)
BUT LOWER PRESSURE:
3 x 10-6 Torr
(d)
16eV
SAME AS (c)
BUT HIGHER r.f.
POWER:
220W
740
750
760
770
ANALYZING MAGNETIC FIELD (G)

ORNL-DWG 89-12492

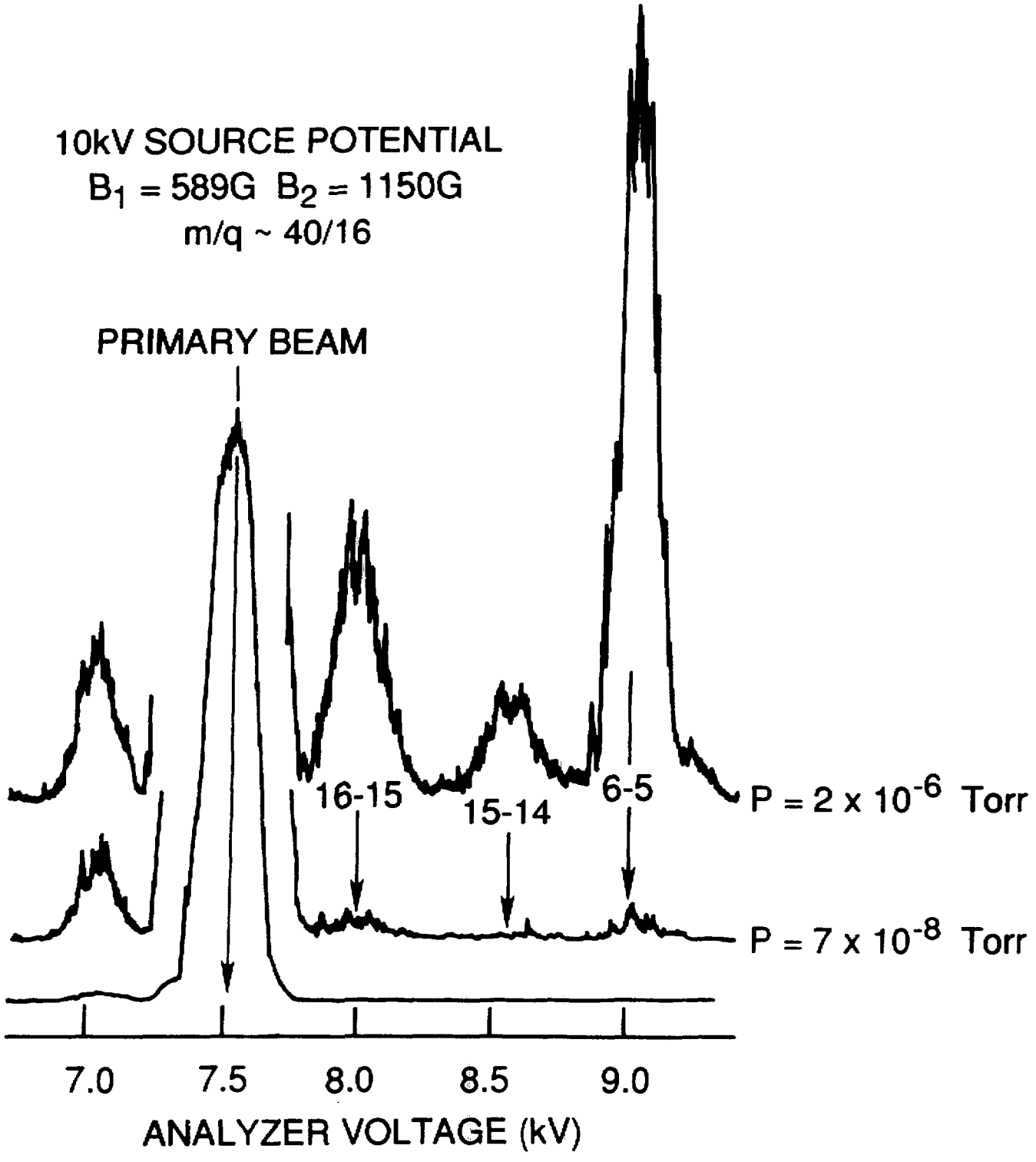

ORNL-DWG 89-12493

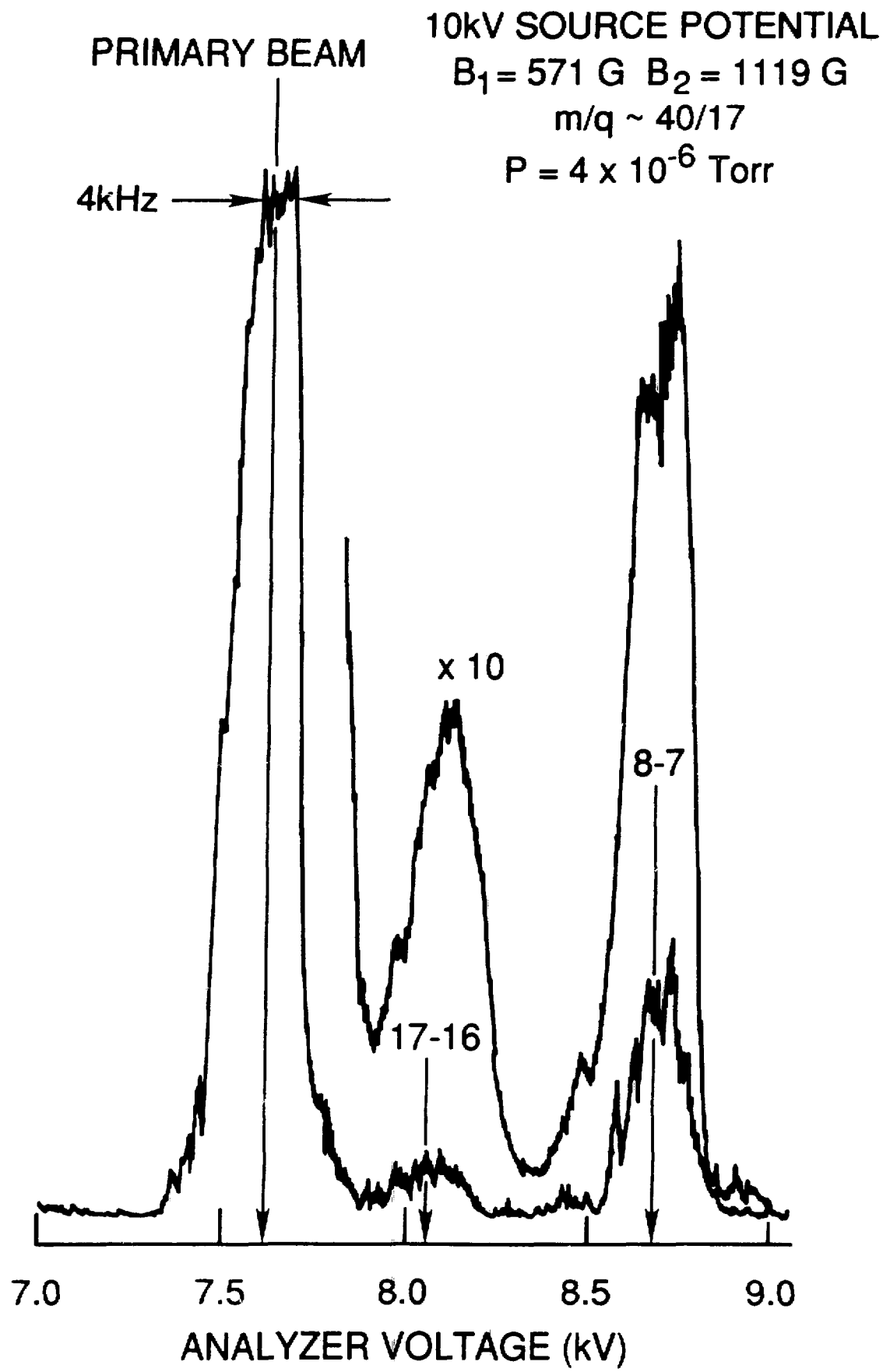

ORNL-DWG 89-12494